Biophysical Chemistry 246 (2019) 16–24

Contents lists available at ScienceDirect

Biophysical Chemistry

journal homepage: www.elsevier.com/locate/biophyschem

Ab initio model for the chlorophyll-lutein exciton coupling in the LHCII complex

Daniil Khokhlov*, Aleksandr Belov

Department of Chemistry, Lomonosov Moscow State University, Leninskie gory 1–3, Moscow 119991, Russia

HIGHLIGHTS

- Active space must include the entire π-system of lutein in MCSCF calculations.
- S_1-S_1 exciton coupling in the Lut620/Chla612 dimer in LHCII is 21.9 cm^{-1} (unscaled).
- Rotations of pigments in the dimer do not change exciton coupling significantly.
- Interplane distance between pigments in the dimer should change in NPQ regulation.

GRAPHICAL ABSTRACT

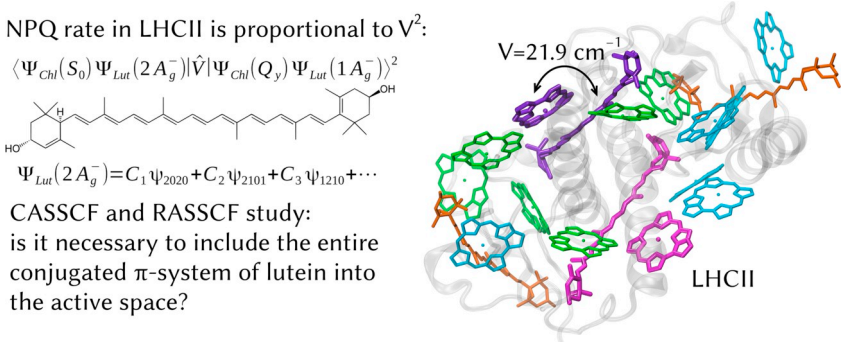

ARTICLE INFO

Keywords:
Xanthophyll
Lutein
LHCII
Non-photochemical quenching
Exciton coupling
MCSCF

ABSTRACT

$2A_g^-$ state of lutein plays a crucial role in photoprotection of higher plants. Due to its multiconfigurational nature, accurate description of this electronic state and respective transition properties is a formidable task. In this paper, applicability of various CASSCF and RASSCF formulations for description of the $2A_g^-$ state is discussed. It is shown that inclusion of the entire π-system of lutein into the active space is required for accurate calculation of transition properties. Exciton coupling in the chlorophyll-lutein dimer involved in non-photochemical quenching in the LHCII complex was calculated to provide a connection between pigment interactions and non-photochemical quenching regulation.

1. Introduction

Non-photochemical quenching of chlorophyll fluorescence is an important part of the protection of photosynthetic apparatus from degradation under excessive light. In such conditions, reaction centers are unable to convert all excitation energy into chemical one which leads to formation of various strong oxidizers such as the long-lived special pair radical $P_{680}^{+\bullet}$ and singlet oxygen $^1\Delta_gO_2$ [1,2]. They could irreversibly damage protein environment and/or pigments thereby disrupting normal functioning of the photosynthetic apparatus. In photosystem II (PSII) of higher plants, almost all peripheral antennae such as CP24, CP26, CP29, and LHCII proteins could serve as fluorescence quenching sites. The latter acts as a light-harvesting antenna most of the time while under high-light conditions it is an important fluorescence quencher.

All these proteins bind various xanthophylls (oxygenated carotenoids) such as lutein, zeaxanthin, neoxanthin and violaxanthin. Xanthophylls play at least three different roles in photosynthetic complexes: they stabilize protein structure, absorb light in blue spectral region, and take part in non-photochemical quenching (NPQ) of

* Corresponding author.
E-mail address: daniilkh@phys.chem.msu.ru (D. Khokhlov).

https://doi.org/10.1016/j.bpc.2019.01.001
Received 25 October 2018; Received in revised form 27 December 2018; Accepted 2 January 2019
Available online 03 January 2019

chlorophyll fluorescence [3]. Two notable properties of xanthophylls make them powerful quenchers of chlorophyll fluorescence. First, energy-wise the S_1 state ($2A_g^-$ assuming ideal C_{2h} polyene symmetry [4]) of some xanthophylls such as lutein and zeaxanthin lies below the S_1 state of chlorophyll *a* (Q_y transition in Gouterman model [5]), thus making the excitation energy transfer from the pool of chlorophylls *a* to the lutein molecule possible [6,7]. Second, the $2A_g^-$ state of xanthophylls promptly (lifetime ~10–25 ps [8]) decays to the ground state ($1A_g^-$) *via* radiationless internal conversion providing the way to trap excessive excitation energy. Therefore, the excitation pathway may look as follows [9]: rapid energy transfer from chlorophylls *b* (less than 1 ps [10]) and energy equilibration in the pool of chlorophylls *a* (several ps [11]) are followed by a relatively slow energy transfer (from 130 ps for quenched LHCII to 1 ns for unquenched one [12]) to one of the xanthophylls in the complex with a subsequent fast relaxation to its $1A_g^-$ state.

For the LHCII complex, this model was extensively developed by theoretical means by Duffy and coworkers [13,14,15]. The closely packed heterodimer of lutein #620 and chlorophyll *a* #612 (further denoted as Lut620/Chla612 dimer, hereinafter numbering according to PDB ID: 1RWT [16]) is supposed to be the quenching site in the LHCII protein due to a relatively large interaction energy between the ground and the lowest excited states of both pigments in the pair (exciton coupling ~14 cm^{-1} [13]). Exciton couplings of Lut620 with other chlorophylls can be considered to be negligible. Further, this model was expanded to the entire LHCII complex by including both chlorophylls and xanthophylls into the exciton Hamiltonian. It confirmed the previously supposed quenching pathway [14]. LHCII contains yet another closely coupled Lut621/Chla603 dimer (Fig. 1) which can take part in energy trapping. However, this lutein is coupled with chlorophylls *a* #602/603/604 with higher excitation energies than chlorophylls #610/612/613 which are known to have the lowest excitation energies in the complex [17]. Thus, taking into account rapid excitation equilibration in the chlorophyll *a* pool, the quenching pathway through Lut620/Chla612 looks more probable. Moreover, the same model was successfully used to describe switching in LHCII from the light-harvesting state to the quenching one [15]. Mutual rotations of the pigments in the dimer lead to significant change of transition density overlap and, thus, may promote NPQ in LHCII.

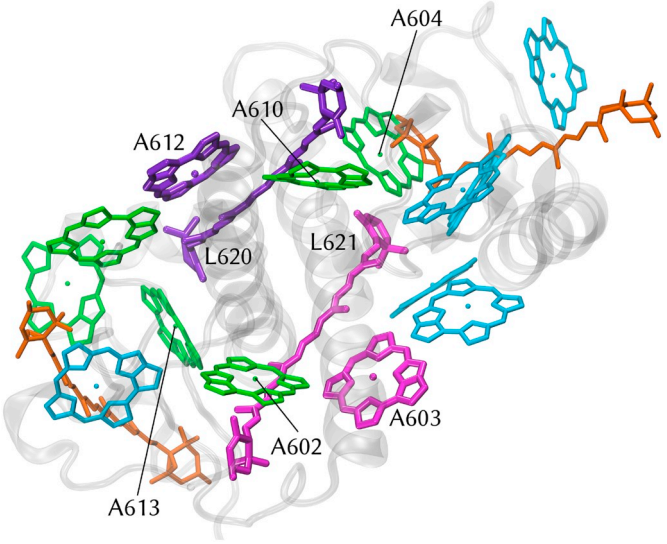

Fig. 1. Structure of the LHCII complex of *Spinacia oleracea* (from PDB ID: 1RWT). Protein is shown in gray, chlorophylls *a* and *b* – in green and cyan, respectively. Neoxanthin and violaxanthin are shown in orange. The two closely packed dimers Lut620/Chla612 and Lut621/Chla603 are shown in magenta and violet, respectively. Image was prepared in VMD program [18]. (For interpretation of the references to color in this figure legend, the reader is referred to the web version of this article.)

While the Q_y state of chlorophyll *a* is dominated by HOMO → LUMO excitation [19] and, thus, can be accurately described by many quantum chemical approaches from time-dependent functional theory (TD-DFT) to various formulations of multireference perturbation theories, the $2A_g^-$ state of lutein has a more complicated electronic structure due to its multiconfigurational nature [4,20]. Semiempirical multiconfigurational methods has been used for calculations in the early works of 70s and 80s [21,4] and are still in use [20,22,15]. The canonical TD-DFT approach yields a relatively good excitation energy (2.18 eV as compared to the experimental value of 1.76 eV [7]) due to a fortunate cancellation of errors [23] but a poor transition dipole value (11.9 times higher than DFT/MRCI reference in the same work) since this method is single reference by design. A more sophisticated semiemprical DFT/MRCI approach adopting DFT terms in the MRCI Hamiltonian was successfully used for calculation of excitation energies of xanthophylls [24] including lutein [25,23]. *Ab initio* methods based on density matrix renormalization group *ansatz* (DMRG) which accounts for static correlation in large active spaces were successfully applied to large polyenes including carotenoids. They give correct energetic ordering of dark excited states [26] but are not invariant to orbital rotations, thus small transition dipoles can vary significantly depending on orbital choice. Lastly, with regard to photosynthesis, it should be noted that all current NPQ models in the LHCII [13,14,15] complex rely on semiempirical CAS-CI calculations for the lutein molecule and, thus, may be refined by *ab initio* means.

In this paper, an *ab initio* study of the exciton coupling in the Lut620/Chla612 pigment pair is presented. The paper is organized as follows. First, impact of the active space choice and wavefunction size in the MCSCF calculation on the electronic properties of the $2A_g^-$ state of the lutein molecule is discussed. Second, exciton coupling in the Lut620/Chla612 pair is calculated basing on the results for the individual pigments. Last, the influence of mutual orientations of the pigments in the pair on the exciton coupling is studied for internal coordinates which may be involved in NPQ regulation in the LHCII complex. The obtained *ab initio* results are compared to the semi-empirical ones following the approaches reported previously.

2. Computation details

2.1. Individual pigments

2.1.1. Lutein

Initial positions of heavy atoms in the lutein molecule were taken from the X-ray structure of the LHCII complex of *Spinacia oleracea* (PDB ID: 1RWT [16]), namely the lutein #620 was used. After addition of hydrogen atoms, geometry was optimized at DFT/B3LYP/6-31G* level. RMSD of conjugated bond lengths compared to the X-ray structure of lutein ester [27] is $8.4 \cdot 10^{-3}$ Å with maximum deviation $1.8 \cdot 10^{-2}$ Å.

Starting molecular orbitals (MOs) for the MCSCF calculations were prepared in the following way. In order to obtain initial approximation, Hartree-Fock calculation was carried out in minimalistic ANO-S-MB basis set lacking orbitals with angular momentum quantum number higher than 1 to facilitate identification of virtual orbitals of π-symmetry. Further, MP2 correction was applied to the previous calculation, and natural orbitals were obtained from the MP2 reduced density matrix. We selected MOs corresponding to the conjugated π-system of the lutein molecule and projected them onto the larger ANO-L-VDZP basis set designed for accurate description of electronic properties with correlated wavefunctions [28]. Thus, the obtained MOs had proper symmetry but they were not optimized in the new basis set. State-specific ($1A_g^-$ state only was included) restricted active space SCF (RASSCF [29]) calculation including 20 electrons on 20 orbitals was performed to optimize MOs and protect them against symmetry breaking. In the RASSCF method, the active space is generally split into three subspaces: RAS1 containing only occupied orbitals with limited number of possible

holes, complete active space RAS2, and RAS3 containing only virtual orbital with limited number of allowed electrons. For the calculations described in the paper, we use the following notation for RASSCF active spaces: [A,B,C,X] means that A occupied orbitals are included into RAS1 subspace; B electrons on B orbitals are included into RAS2 subspace; C orbitals are included into RAS3 subspace; X stands for the maximum excitation level allowed from RAS1 and to RAS3 ("s" for single excitations,"sd" for singles and doubles). Following this notation, in preparation of MOs, active space of the type [10,0,10,sd] was used. The optimized MOs obtained in this procedure (fig. S1) were used as a starting guess in all further calculations for the lutein molecule.

Complete active space SCF (CASSCF) and RASSCF with various active spaces were used to calculate transition dipole moments and density matrices corresponding to the transition from the $1A_g^-$ to the $2A_g^-$ state. State-averaged formulation of MCSCF was used to provide a balanced description of $1A_g^-$ and $2A_g^-$ states simultaneously; both states had equal weights in the averaging. Within the CASSCF approach we studied symmetric active spaces (referred to as [N_{el}, N_{orb}]) with sizes from [6,6] to [14,14]. The latter space is close to the current computational limit and, thus, CASSCF does not allow inclusion of the entire conjugated π-system of lutein which would be desirable. RASSCF is able to overcome this limitation, so it was used to study effects of static correlation in the entire π-system. Each choice of active space for RASSCF contained 20 electrons on 20 orbitals shared by three RASSCF subspaces: RAS2 contained equal number of electrons and orbitals and the remaining orbitals were equally distributed between RAS1 and RAS3 subspaces. We used two different sets of active spaces in RASSCF: in the first one (referred to as RAS(s)), only single excitations were allowed from RAS1 and to RAS3; in the second one (referred to as RAS (sd)), single and double excitations were allowed from RAS1 and to RAS3. So, the active spaces used were of the type [10-N/2,N,10-N/2,s or sd] where N varied from 4 to 8.

2.1.2. Chlorophyll a

Geometry optimization procedure was the same as for the lutein molecule; chlorophyll *a* #612 was taken from the same PDB. Nonpolar phytyl tail was replaced by methyl group in all quantum chemical calculations in order to accelerate them since it does not affect the π-system. RASSCF was used for calculation of electronic properties of the chlorophyll in order to achieve consistency with quantum chemical description of the lutein molecule. Starting MOs for MCSCF calculations were prepared by projecting the Hartree-Fock orbitals obtained in ANO-S-MB basis set into ANO-L-VDZP. 20 orbitals corresponding to the conjugated π-system of the chlorin ring (fig. S2) were selected. RASSCF active space was [8,4,8,sd]. The three lowest electronic states (ground, Q_y, and Q_x) were included in state-averaging with equal weights. Resulting transition dipole between the ground and the Q_y states is 5.46 D and agrees well with the experimental one (4.49 D) obtained from extrapolation of experimental transition dipoles to vacuum permittivity [30]. Therefore, transition densities were used further without any rescaling. However, it should be noted that proper rescaling of chlorophyll *a* dipole can lead to decreasing of the exciton coupling by a factor of 0.82.

2.1.3. Software

Geometry optimizations were performed using GAMESS-US [33]. Preparation of MOs and MCSCF calculations were performed in OpenMolcas (build #180705–1750), the developer's version of MOLCAS package [34]. In the OpenMolcas calculations, Cholesky decomposition (using default decomposition threshold $1.0 \cdot 10-4$) of two-electron integrals in combination with atomic compact auxiliary basis set [35] was used to accelerate calculations. Transition dipole moments were calculated in dipole-length formulation.

2.2. Semi-empirical CAS-CI

Semi-empirical AM1-CAS-CI calculations were performed in MOPAC2016 [31] on the same geometries of pigments as for *ab initio* calculations; complete active space included 6 electrons on 6 orbitals for both pigments. In the calculation of the lutein molecule, the SCF procedure that preceded CI was carried out with unitary occupancies for molecular orbitals of CI active space following the computation protocol described in [22]. Since semi-empirical methods lack explicit analytic form for wavefunctions, the respective TrESP charges [41] were calculated on wavefunctions obtained *via* projecting the implied orthogonal basis onto STO-6G basis set using Löwdin "deorthogonalization" procedure in the same way as it is implemented in MOPAC for ESP charges [32]. Rescaling of transition densities was not made to be consistent with our *ab initio* results.

2.3. Structure of the chlorophyll-lutein pigment pair

Initial structure of the subunit of the LHCII complex (chain A) was taken from PDB ID: 1RWT [16]. Hydrogen atoms were added; protonation states of amino acids were the default ones for physiological pH; all histidine residues were in δ-configurations. After addition of hydrogen atoms, protein was placed in the explicit 10 Å truncated octahedral water box; the system was neutralized by adding 12 sodium ions to the simulation box. Solvent box was optimized (atoms of the complex and ions were frozen) using 10,000 steps of steepest descent algorithm. Further optimization was carried out for the entire system using conjugated gradient algorithm with double accuracy. RMSD between the coordinates of heavy atoms of the dimer in the optimized structure and that in the X-ray structure was 0.66 Å. All molecular mechanics calculations were performed in AMBER18 package [36], AMBER10 force field was used for proteins, AMBER-compatible force fields for chlorophylls and xanthophylls [37,38], generalized AMBER force field [39] for LHG phospholipid, and TIP3P model [40] for water.

2.4. Exciton coupling between pigments

Exciton coupling $V_{Lut-Chl}$ between the two transition densities from the ground to the first excited states for both pigments reads

$$V_{Lut-Chl} = \left\langle \psi_e^{Lut}\psi_g^{Chl} \mid \hat{V} \mid \psi_g^{Lut}\psi_e^{Chl} \right\rangle, \quad (1)$$

where $\hat{V}$ – Coulomb interaction operator, ψ_g^{Lut} and ψ_e^{Lut} – wavefunctions of the $1A_g^-$ and $2A_g^-$ states of lutein, respectively, ψ_g^{Chl} and ψ_e^{Chl} – wavefunctions of the ground and the Q_y states of chlorophyll, respectively. For coupling calculation, an approximate approach based on effective TrESP (transition ESP) charges [41] located on the nuclei and fitted to non-diagonal matrix elements of electrostatic potential operator was used. This approach for coupling calculation was chosen for the sake of transferability of the charges to another geometries of the pigment (provided they are not too different) which is an advantage over other methods such as transition density cubes [42] or cumulative atomic multipole moments [43]. Although such transferability is limited to small distortions of the structure of pigment, the reported transition charges can be useful for further NPQ studies. The resulting drawback *i.e.* inability to describe the component of transition dipole which is orthogonal to the π-system plane is not significant since the transition density is symmetric with respect to the plane for π-π transitions. In this method, exciton coupling can be evaluated as Coulomb interaction energy between two sets of TrESP charges q^{Lut} and q^{Chl}, corresponding to transitions under consideration in lutein and chlorophyll:

$$V_{Lut-Chl} \simeq \sum_{i,j} \frac{q_i^{Lut} q_j^{Chl}}{\left| \overrightarrow{R}_i^{Lut} - \overrightarrow{R}_j^{Chl} \right|}, \quad (2)$$

where summation is carried out over all charges in the set, $\overrightarrow{R}_i^{Lut}$ and $\overrightarrow{R}_i^{Chl}$ – positions of the corresponding charges. TrESP charges were evaluated by fitting electrostatic potential calculated on a geodesic grid surrounding nuclei using in-house software and transition density matrices from MCSCF calculations. Effective charges calculated for the *in vacuo* optimized structures were placed in the positions of the corresponding atoms in the MM structure. Direct fitting of the QM structures of the entire pigment molecules into the MM geometry of the dimer (as is and with internal rotations, see Section 3.3) was also tested (see Supplementary, section S2) However, sterical clashes of the side groups lead to unstable behavior at large rotation angles.

3. Results and discussion

3.1. Transition properties of the lutein molecule

Since we are interested in exciton coupling between the $1A_g^- \rightarrow 2A_g^-$ transition in the lutein and the $S_0 \rightarrow Q_y$ transition in the chlorophyll *a*, we started with the study of transition electronic properties of the individual pigments. Excited state of chlorophyll *a* can be described with appropriate accuracy with a modest computational effort (Section 2.1.2), therefore, we focused on the lutein molecule. First, systematical study of the impact of the active space size on the electronic properties of the lutein molecule within MCSCF framework was done. CASSCF in relatively small active spaces (up to [14,14]) is promising from the viewpoint of further improvement of energies and, to a much lesser extent, of transition properties using multireference perturbation theories. $2A_g^-$ state wavefunction is dominated by three CSFs (ϕ_{2101}, ϕ_{1210}, and ϕ_{2020}; index in the subscript consists of the two highest occupied orbitals and the two lowest unoccupied) which can be captured even by a small active space. However, expansion of the active space does not lead to convergent transition dipole values which do not have monotonous dependence on the active space size (Table 1). Deviation from C_{2h} symmetry in the lutein molecule leads to orbital symmetry breaking (deviation from or complete absence of the symmetry of an orbital as compared to the expected one of a linear polyene) for several occupied and unoccupied MOs which seems to be the main reason for such behavior. MOs from 6 to 4 (occupied orbitals are numbered from 10 to 1 in ascending order of orbital occupancy in the initial SS-RASSCF, unoccupied orbitals – from 1′ to 10′ in descending order of orbitals occupancy in the same calculation) and the corresponding unoccupied ones are the product of mixing of MOs of ideal 9-ene with the π-orbital of cyclohexene ring (Fig. 2) which is pulled out of the conjugated π-system by 48 degrees and, thus, has a small overlap with it. The [6,6] active space contains doubly occupied MOs from 3 to 1 and does not have any orbitals mixed with the out-of-plane π-orbital. Thus, the results of MCSCF closely resemble (fig. S3) that for an ideal polyene with the forbidden $1A_g^- \rightarrow 2A_g^-$ transition which leads to underestimation of transition dipole value ($9{\cdot}10^{-3}$ D). Further expansion of the active space gradually incorporates MOs with broken symmetry which, in absence of lower lying orbitals, destabilize MCSCF solution which produce MOs substantially localized in the cyclohexene π-system (fig. S4). In this case, the wavefunction of the $2A_g^-$ state is contaminated by ϕ_{2110} CSF of B_u symmetry (table S1) which has non-zero contribution to transition dipole matrix elements $\left\langle \Psi_{1A_g^-} \mid \hat{d} \mid \phi_{2110} \right\rangle$. This affects the transition dipole value which gradually increases upon inclusion of new orbitals of broken symmetry(from 0.61 to 0.71 D). The orbital 7 (Fig. 2) has a nearly ideal C_{2h} symmetry due to small contribution from the cyclohexene π-orbital. When included into the active space (CASSCF[14,14]), it changes the behavior of MCSCF procedure again decreasing transition dipole down to $6.2{\cdot}10^{-2}$ D. Basing only on CASSCF results, any reliable conclusions could not be made about the transition dipole value due to the technical impossibility of further expansion of complete active space. The main question is whether the transition dipole value is close to the CASSCF[8,8]-CASSCF[12,12] results or the CASSCF[14,14] result. The lack of experimental data does not allow to make a conclusion at this step, thus, active space should be expanded in some way. Even in the case of the largest CASSCF[14,14] the occupancies of the orbitals with the highest occupancies and with the lowest ones for $2A_g^-$ state are far (table S2) from common criteria for exclusion of orbitals from active space (> 1.98 and < 0.02, respectively [45]) which emphasizes the importance of further active space expansion.

The entire conjugated π-system of lutein was treated using RASSCF formalism which can deal with large active spaces with restricted electronic excitations. RAS2 active space was systematically expanded while RAS1 and RAS3 contained the remaining MOs (for details see Section 2.1.1). MCSCF calculations with the smallest RAS2 active space (4 orbitals) produced much higher dipole values than the others possibly due to impossibility to incorporate all significant CSFs. Expansion of RAS2 leads to substantial decrease of transition dipole moment which has the same order of magnitude as in CASSCF[14,14]. Also, in all studied active spaces (Table 1), RASSCF with higher number of holes in RAS1/electrons in RAS3 gave higher dipole values reflecting higher contribution from broken symmetry orbitals. In the absence of experimental reference, it is interesting to compare the MCSCF transition dipole values with those from other computational methods. Values obtained by RASSCF method with large active spaces (0.03–0.07 D) deviate significantly (by one order of magnitude) from the DFT/MRCI result (0.767 D [23]). However, DFT/MRCI is known to yield the results different from those of the state-of-the-art references such as multireference perturbation theories, especially for dipole-forbidden transitions, and such references are absent for xanthophylls. It should be noted that RASSCF can not serve as such reference. First, it does not account for static correlation in the π-system to the same extent as the CASSCF with the entire π-system included into the active space due to the limited number of excitations from the RAS1 to the RAS3 subspace. Second, it lacks any dynamic correlation contribution. The latter factor, however, has more effect on the energy value and less so on the electron density.

3.2. Exciton coupling in the pigment pair

Exciton coupling $V_{Lut-Chl}$ in the Lut620/Chla612 dimer relevant to NPQ in LHCII was calculated as described in Section 2.4. The coupling depends on the active space size to a much lesser extent than the

Table 1
Excitation energies and norms of transition dipole moments between the ground and the $2A_g^-$ electronic states of the lutein molecule obtained in various active spaces.

CAS size	CAS		RAS2 size	RAS(s)		RAS(sd)	
	ΔE_{01}, eV	$\lvert\vec{d}_{01}\rvert$, D		ΔE_{01}, eV	$\lvert\vec{d}_{01}\rvert$, D	ΔE_{01}, eV	$\lvert\vec{d}_{01}\rvert$, D
6	4.38	$9.11{\cdot}10^{-3}$	4	3.45	0.156	3.71	0.257
8	4.40	0.612	6	3.36	$2.44{\cdot}10^{-2}$	3.47	$6.76{\cdot}10^{-2}$
10	4.35	0.643	8	3.32	$3.81{\cdot}10^{-2}$	3.35	$5.59{\cdot}10^{-2}$
12	4.26	0.714			–		
14	3.87	$6.20{\cdot}10^{-2}$					

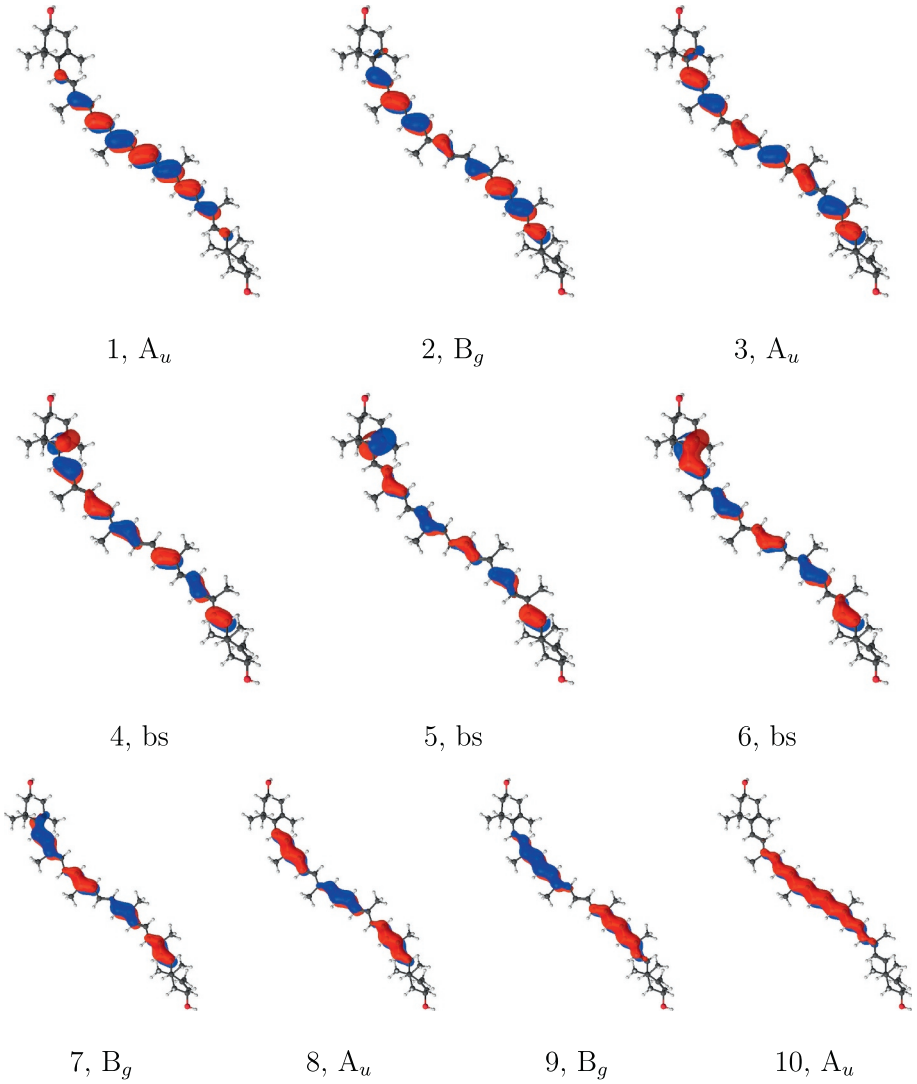

Fig. 2. Occupied active space MOs of the lutein molecule obtained by SS-RASSCF. The same numbering as in the text were used, approximate symmetry in C_{2h} group is indicated. Bs means broken symmetry. MOs were rendered in LUSCUS program [44].

transition dipole moment (Fig. 3) which is due to close proximity of the pigments in the dimer. The pigments reside in parallel planes with interplane distance being approximately 4 Å. In this case, dipole-dipole approximation is not applicable so the coupling is defined by spatial distribution of transition densities. Therefore, similar coupling values indicate that all calculations produce qualitatively the same transition density between the $1A_g^-$ and the $2A_g^-$ states of lutein in the center of the molecule where the distance between the pigments is the smallest. Exciton coupling significantly depends on the distance between the pigments as expected. Increasing the distance between pigments' planes by 3 Å is enough to decrease the coupling below 10 cm^{-1}.

As can be seen from the Fig. 3, the coupling value converges to a limit with the increasing active space size. Results obtained by RASSCF method within the RAS(s) formulation converge monotonously to the value of 19.2 cm^{-1}. The same is valid for the RAS(sd) results with the limit coupling value being 21.9 cm^{-1}. Although the used active spaces are much smaller than the CASSCF limit for the entire lutein π-system, the nature of convergence implies that the coupling in the limit case would not be very different from the results obtained by RASSCF with large active spaces. Such relatively large value (for a coupling with a dipole-forbidden state) gives additional support to the hypothesis that LHCII is in a highly quenched state in its X-ray conformation [46]. Direct comparison of exciton coupling with previous papers is not possible due to slightly different pigment pair geometries. This value is much higher than the value of 2 cm^{-1} reported by Balevicius et al. [15] and higher than the same coupling calculated with MNDO-CAS-CI [13] by a factor of 1.6 which can be explained by the difference in computational methods and the dimer geometries. To eliminate the geometry factor, semi-empirical calculations on the same dimer geometries were carried out; the results are reported in Section 3.3.3.

3.3. Chlorophyll - lutein exciton coupling as a function of internal coordinates

Dependence of the coupling in the Lut620/Chla612 dimer on the relative positions of the pigments is essential for NPQ regulation mechanism. Two internal movements in the dimer, namely the rotation of the lutein molecule in the plane parallel to the chlorophyll molecule and the angle change between the lutein axis and the chlorophyll plane, are supposed to be involved in NPQ control in the LHCII antenna [15]. Basing on the *ab initio* model for the coupling, its dependence on three internal coordinates including the two noted above is discussed further (for exact definitions of rotation angles see Supplementary, section S4). Apart from regulatory implications of such dependence, the study is aimed to discriminate between various MCSCF formulations with regards to the transition density distributions along the lutein molecule.

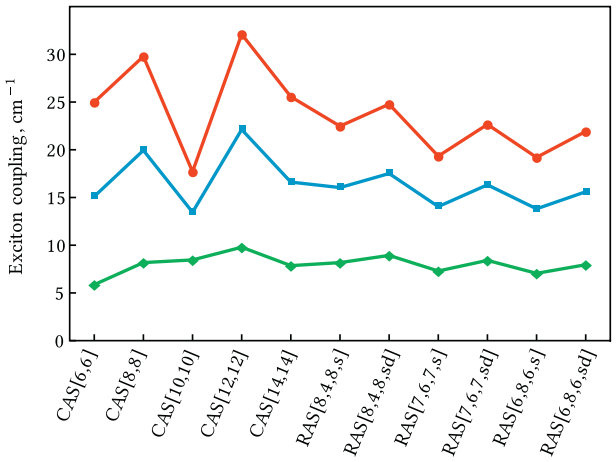

Fig. 3. Exciton coupling $V_{Lut-Chl}$ calculated on the various TrESP charges for lutein. Red line corresponds to the MM equilibrium geometry of the pigment dimer in the LHCII complex. Blue line corresponds to the pigments in the dimer pair pushed apart by 1 Å with respect to equilibrium geometry, green one – pushed by 3 Å. Active space size in CASSCF and RASSCF is given in brackets. (For interpretation of the references to color in this figure legend, the reader is referred to the web version of this article.)

3.3.1. Rotation of the chlorophyll molecule

The first coordinate is the angle of rotation of the chlorophyll *a* molecule within its plane around the axis centered at magnesium atom. This coordinate is not directly related to NPQ activation but has a significant impact on the coupling (Fig. 4) due to that the chlorophyll transition density is mostly located on the B ring close to the lutein molecule (the corresponding TrESP charges are provided in Supplementary, fig. S7).

Exciton couplings calculated basing on CASSCF exhibit inconsistent behavior (Fig. 4b) upon expansion of the active space. Two active spaces, namely [8,8] and [12,12], produce similar transition density distributions as indicated by similar coupling plots. Three other spaces, namely [6,6], [10,10], and [14,14], produce the angle-coupling functions dissimilar to one another as well as to the previous two. This can be viewed as an additional evidence that CASSCF with small active space is not capable to describe the $2A_g^-$ state of the lutein molecule properly. Therefore, any CASSCF-based conclusions regarding the NPQ rate in the chlorophyll-lutein dimer should be treated with caution.

The angle-coupling dependences for RASSCF density matrices exhibit a more stable behavior upon expansion of the active space (Fig. 4c). Within the rotation angle range of ± 90 degrees, the mean deviation between the couplings for RAS spaces of different size is 6.46 ± 2.68 cm^{-1}. If the two smallest RASSCF spaces, namely [8,4,8,s] and [8,4,8,sd], are excluded, the deviation decreases to 3.57 ± 1.03 cm^{-1}. This shows that RASSCF method for active spaces of different sizes gives internally consistent results which approach a limit when the number of CSFs grows thus providing reliable transition densities.

3.3.2. Rotations of the lutein molecule

Two internal coordinates were studied: a) angle of rotation of the lutein molecule in the plane of its own π-system with respect to the axis centered on the middle of the C15-C35 bond and b) tilt angle of the lutein π-system axis with respect to the chlorophyll molecule plane (see Fig. 5a, c). These two coordinates are supposed to be involved in NPQ activation [15].

Considering the instability of CASSCF-based results shown previously, we focused on RASSCF. It can be seen from Fig. 5b, d that exciton couplings have a moderate dependence on these internal coordinates and behave consistently for active spaces of different sizes. In-plane rotation of lutein by 35 degrees leads to significant increase of the exciton coupling (up to 32 cm^{-1} in [6,8,6,sd]) but it is not clear whether the dimer can really adopt such conformation. Assuming that ± 20 degrees range of rotation and tilt angles from the equilibrium value is accessible in the real protein (for the tilt angle even that would be an overestimation due to Chl-Lut sterical clashes), the range of possible coupling values in the dimer is rather narrow. Within the said range of the in-plane rotation angle, with the RASSCF active spaces [8,4,8,s] and [8,4,8,sd] excluded, the coupling value falls in the range between 19 and 24 cm^{-1}. Within the same range of the tilt angle, the coupling stays in the range from 18 to 24 cm^{-1}. This result contrasts

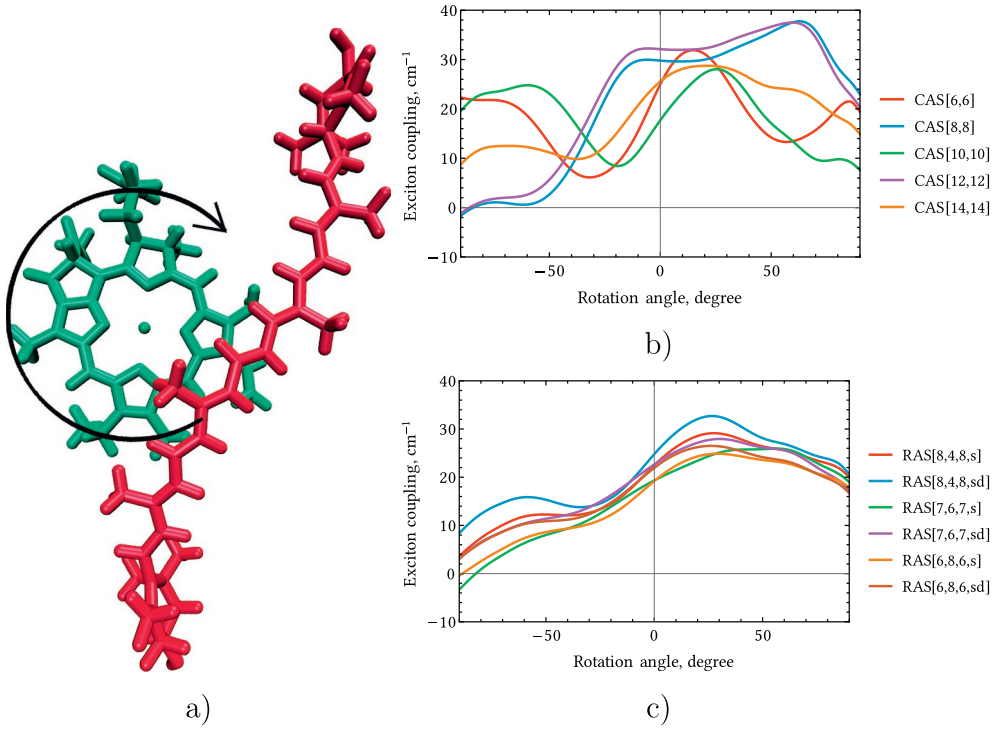

Fig. 4. Internal coordinate #1 – in-plane rotation of the chlorophyll *a* molecule. a) Structure of the Lut620/Chla612 dimer. Chlorophyll is shown in green, lutein – in red. Arrow shows the direction of the pigment rotation. b,c) Exciton coupling as a function of the chlorophyll rotation angle calculated based on CASSCF (b) or RASSCF (c). (For interpretation of the references to color in this figure legend, the reader is referred to the web version of this article.)

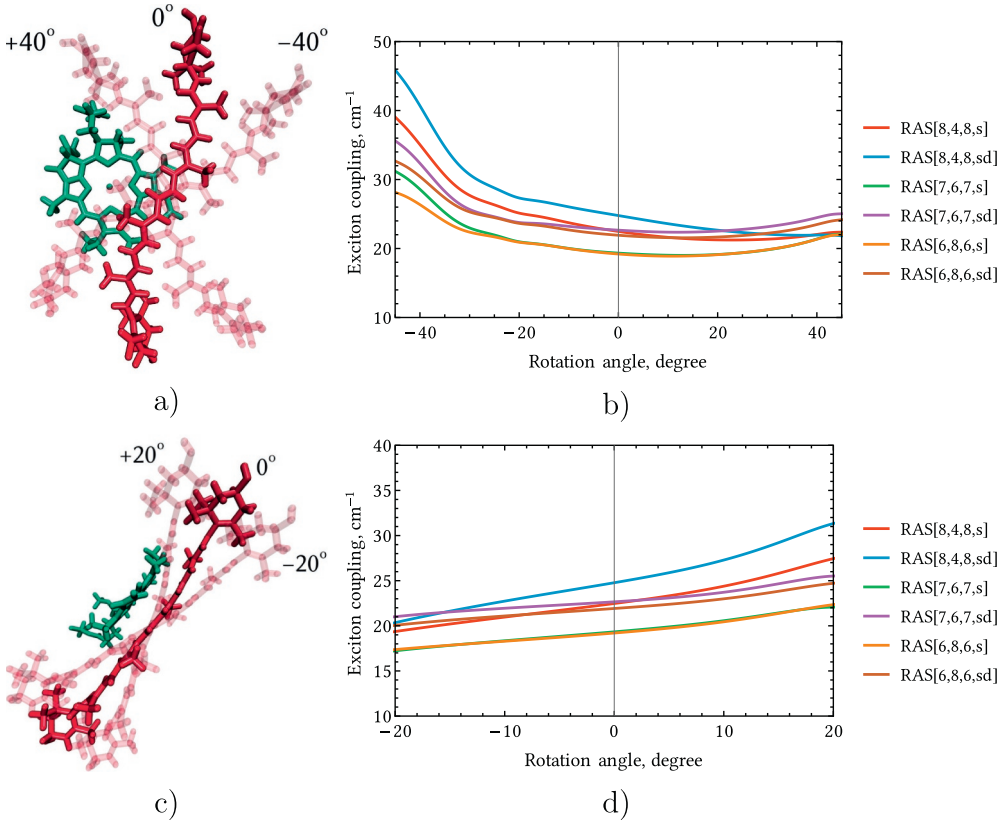

Fig. 5. Internal coordinates #2 and #3 – in-plane and out-of-plane rotation of the lutein *a* molecule. a,c) Structure of the Lut620/Chla612 dimer. Chlorophyll is shown in green, lutein – in red; translucent lutein molecules indicate the range of angles. b,d) RASSCF-based exciton couplings as a function of b) in-plane rotation angle and d) out-of-plane tilt angle. (For interpretation of the references to color in this figure legend, the reader is referred to the web version of this article.)

with a more pronounced angle-coupling dependence obtained by the AM1-CAS-CI method [15]. Moreover, rotation and tilt-related variations of exciton coupling are much lower than that introduced by the change of the interplane distance which is likely accompany any structural change within the Lut620/Chla612 dimer. Nevertheless, all internal movements in the pigment pair combined can have a significant impact on the exciton coupling and, thus, underlie the NPQ regulation in the LHCII complex.

3.3.3. Comparison with the semi-empirical model

The same coupling-angle plots were calculated using AM1-CAS-CI to estimate the impact of the computational method on the model of NPQ process. The obtained semi-empirical coupling-angle plot for chlorophyll rotation (Fig. 6, red line) is in a qualitative agreement with the one provided in the paper of Balevicius et al. [15]: it reproduces all specific features such as the minimum near −120 degrees, the broad

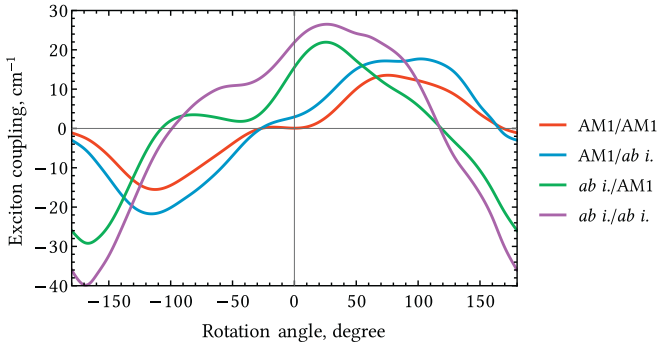

Fig. 6. Exciton coupling as a function of rotation angle of the chlorophyll molecule (as described above, Fig. 4a). A/B denotes computational method for lutein/chlorophyll, respectively. AM1 stands for AM1-CAS-CI, *ab i.* stands for RASSCF in the largest active space [6,8,6,sd].

maximum near 70 degrees, and the plateau near 0 degrees. The difference of the maximal positive coupling value (~13 cm^{-1}*versus* ~20 cm^{-1}) arises predominantly from the absence of rescaling in our model and much less from the difference of geometries. Indeed, if rescaling factor 1.67 (taken from supplementary of [15]), maximal positive value of the coupling becomes 22 cm^{-1} which is much closer to the cited value. Since the geometry difference cannot be eliminated completely, further discussion will focus on the results obtained using our geometry.

In the range of physiologically accessible rotation angles AM1-CAS-CI and RASSCF couplings (Fig. 6, red and purple lines, respectively) behave differently. While the semi-empirical values are close to zero and can vary severalfold, the *ab initio* couplings are already relatively large (for this system) in the equilibrium geometry and can vary by no more that two times. This facts support the hypothesis that the change of the interpigment distance in the dimer is important for NPQ. However, it should be noted that the volume change corresponding to the transition to the quenched state is very small (~0.006% [47]) which limits the contribution of the interpigment distance change in the NPQ activation.

It can be useful to calculate exciton couplings basing on *ab initio* TrESP charges for one pigment and semi-emprical ones for another pigment. Although, it produces inconsistent and, thus, unphysical coupling it can be used to find out which pigment requires computationally demanding *ab initio* treatment to produce accurate results. If the chlorophyll only is described by AM1-CAS-CI (Fig. 6, green line), the coupling-angle dependence is much closer to the RASSCF plot than one for the semi-empirically modeled lutein. This is in complete agreement with the fact that the HOMO→LUMO transition in chlorophyll is much easier to describe accurately than the transition from the ground to the multiconfigurational $2A_g^-$ state of the lutein molecule and emphasizes the importance of the accurate model for electronic structure of lutein. The two methods produce transition densities which are located differently within the lutein molecule. For AM1, transition density is localized on one end of the π-system which is far from the

Chl-Lut contact region. So, a significant rotation angle is required to achieve considerable coupling. For RASSCF, transition density is distributed more evenly, has an inversion pseudosymmetry and produces the TrESP charges which are nonzero in the region of close contact. The visualization of TrESP charges derived from AM1 and the largest RASSCF for both pigments is provided in the Supplementary (fig. S7). The plots for the two remaining internal coordinates (rotations of lutein) exhibit the behavior similar to the one for chlorophyll rotation (near-zero values for AM1 and nonzero values for *ab initio* at equilibrium geometry) and are less representative, thus they are shown in Supplementary (fig. S8).

4. Conclusion

Multiconfigurational nature of the dark $2A_g^-$ of the lutein molecule makes it necessary to use multireference methods for its accurate description. As shown in this paper, it is also necessary to include the entire conjugated π-system of lutein into the active space which makes the computational effort required to perform a CASSCF calculation prohibitive. Thus, multireference methods using incomplete active spaces with an appropriate method for CSF selection are necessary for such calculations. With active spaces of moderate sizes, the RASSCF method yields consistent $1A_g^- \rightarrow 2A_g^-$ transition properties including transition dipole and transition density. Basing on the RASSCF results, the value of exciton coupling in the Lut620/Chla612 dimer in the LHCII complex was found to be 21.9 cm^{-1}. This value is much higher than the MNDO/AM1-CAS-CI results reported previously [13,15]. Moreover, the sensitivity of this coupling to internal movements in the dimer, namely the lutein rotation and tilt angles, is quite different within RASSCF and semi-empirical approaches. Due to high sensitivity of lutein transition properties to the choice of computational method, any conclusions regarding exciton coupling value should be made cautiously. Since the excitation energy transfer rate has a quadratic dependence on the coupling, the latter consideration is also important in studying of NPQ regulation. Despite the supposed accuracy of the reported *ab initio* methods, they have a major drawback, namely the prohibitive computational complexity when applied to multiple frames of MD trajectories. We suppose that this problem can be addressed either by some parametrization of transitional electronic density of the pigments which accounts for changes of their geometries or by reducing the phase space in MD to a limited set of conformations. For this, further research is required.

Acknowledgements

This work was supported by Russian Foundation for Basic Research [grant number 18-34-00700]. Authors thank Dr. Christopher Duffy (Queen Mary University of London) for insightful discussion about NPQ model and Dr. Ilya Glebov (Lomonosov Moscow State University) for the help with the interpretation of MCSCF results.

Appendix A. Supplementary data

Supplementary data to this article can be found online at https://doi.org/10.1016/j.bpc.2019.01.001.

References

[1] C. Triantaphylidès, M. Havaux, Singlet oxygen in plants: production, detoxification and signaling, Trends Plant Sci. 14 (4) (2009) 219–228, https://doi.org/10.1016/j.tplants.2009.01.008.
[2] I. Vass, Molecular mechanisms of photodamage in the Photosystem II complex, Biochim. Biophys. Acta Bioenerg. 1817 (1) (2012) 209–217, https://doi.org/10.1016/j.bbabio.2011.04.014.
[3] A. Young, G. Britton, Carotenoids in Photosynthesis, Springer Science + Business Media, 1993, https://doi.org/10.1007/978-94-011-2124-8.
[4] P. Tavan, K. Schulten, Electronic excitations in finite and infinite polyenes, Phys. Rev. B 36 (8) (1986) 4337–4358, https://doi.org/10.1103/PhysRevB.36.4337.
[5] M. Gouterman, G.H. Wagnière, L.C. Snyder, Spectra of porphyrins: part II. Four orbital model, J. Mol. Spectrosc. 11 (1–6) (1963) 108–127.
[6] K. Furuichi, T. Sashima, Y. Koyama, The first detection of the 3Ag-state in carotenoids using resonance-Raman excitation profiles, Chem. Phys. Lett. 356 (5–6) (2002) 547–555, https://doi.org/10.1016/S0009-2614(02)00412-8.
[7] P.J. Walla, P.A. Linden, K. Ohta, G.R. Fleming, Excited-state kinetics of the carotenoid S_1 state in LHCII and two-photon excitation spectra of lutein and β-carotene in solution: Efficient Car S_1 Chl electronic energy transfer *via* hot S_1 states? J. Phys. Chem. A 106 (10) (2002) 1909–1916, https://doi.org/10.1021/jp011495.
[8] T. Polívka, V. Sundström, Ultrafast dynamics of carotenoid excited states from solution to natural and artificial systems, Chem. Rev. 104 (2004) 2021–2071, https://doi.org/10.1021/cr020674n.
[9] K.F. Fox, V. Balevičius, J. Chmeliov, L. Valkunas, A.V. Ruban, C.D.P. Duffy, The carotenoid pathway: what is important for excitation quenching in plant antenna complexes? Phys. Chem. Chem. Phys. 19 (34) (2017) 22957–22,968, https://doi.org/10.1039/C7CP03535G.
[10] H. van Amerongen, R. van Grondelle, Understanding the energy transfer function of lhcii, the major light-harvesting complex of green plants, J. Phys. Chem. B 105 (3) (2001) 604–617, https://doi.org/10.1021/jp0028406.
[11] R. Agarwal, B.P. Krueger, G.D. Scholes, M. Yang, J. Yom, L. Mets, G.R. Fleming, Ultrafast energy transfer in lhc-ii revealed by three-pulse photon echo peak shift measurements, J. Phys. Chem. B 104 (13) (2000) 2908–2918, https://doi.org/10.1021/jp9915578.
[12] A.V. Ruban, R. Berera, C. Ilioaia, I.H. Van Stokkum, J.T. Kennis, A.A. Pascal, H. Van Amerongen, B. Robert, P. Horton, R. Van Grondelle, Identification of a mechanism of photoprotective energy dissipation in higher plants, Nature 450 (7169) (2007) 575–578, https://doi.org/10.1038/nature06262.
[13] C.D. Duffy, J. Chmeliov, M. Macernis, J. Sulskus, L. Valkunas, A.V. Ruban, Modeling of fluorescence quenching by lutein in the plant light-harvesting complex LHCII, J. Phys. Chem. B 117 (38) (2013) 10974–10,986, https://doi.org/10.1021/jp3110997.
[14] J. Chmeliov, W.P. Bricker, C. Lo, E. Jouin, L. Valkunas, A.V. Ruban, C.D. Duffy, An 'all pigment' model of excitation quenching in LHCII, Phys. Chem. Chem. Phys. 17 (24) (2015) 15857–15,867, https://doi.org/10.1039/c5cp01905b.
[15] V. Balevičius, K.F. Fox, W.P. Bricker, S. Jurinovich, I.G. Prandi, B. Mennucci, C.D. Duffy, Fine control of chlorophyll-carotenoid interactions defines the functionality of light-harvesting proteins in plants, Sci. Rep. 7 (1) (2017) 1–10, https://doi.org/10.1038/s41598-017-13 (720-6).
[16] Z. Liu, H. Yan, K. Wang, T. Kuang, J. Zhang, L. Gui, X. An, W. Chang, Crystal structure of spinach major light-harvesting complex at 2.72 Å resolution, Nature 428 (6980) (2004) 287–292, https://doi.org/10.1038/nature02373.
[17] V.I. Novoderezhkin, M.A. Palacios, H. Van Amerongen, R. Van Grondelle, Excitation dynamics in the LHCII complex of higher plants: modeling based on the 2.72 Å crystal structure, J. Phys. Chem. B 109 (20) (2005) 10493–10,504, https://doi.org/10.1021/jp044082f.
[18] W. Humphrey, A. Dalke, K. Schulten, VMD: visual molecular dynamics, J. Mol. Graph. 14 (1) (1996) 33–38, https://doi.org/10.1016/0263-7855(96)00018-5.
[19] Z.-L. Cai, M.J. Crossley, J.R. Reimers, R. Kobayashi, R.D. Amos, Density functional theory for charge transfer: the nature of the N-bands of porphyrins and chlorophylls revealed through CAM-B3LYP, CASPT2, and SAC-CI calculations, J. Phys. Chem. B 110 (31) (2006) 15624–15,632, https://doi.org/10.1021/jp063376t.
[20] J.H. Starcke, M. Wormit, J. Schirmer, A. Dreuw, How much double excitation character do the lowest excited states of linear polyenes have? Chem. Phys. 329 (1–3) (2006) 39–49, https://doi.org/10.1016/j.chemphys.2006.07.020.
[21] K. Schulten, M. Karplus, On the origin of a low-lying forbidden transition in polyenes and related molecules, Chem. Phys. Lett. 14 (3) (1972) 305–309, https://doi.org/10.1016/0009-2614(72)80120-9.
[22] M. Macernis, J. Sulskus, C.D.P. Duffy, A.V. Ruban, L. Valkunas, Electronic spectra of structurally deformed lutein, J. Phys. Chem. A 116 (40) (2012) 9843–9853, https://doi.org/10.1021/jp304363q.
[23] O. Andreussi, S. Knecht, C.M. Marian, J. Kongsted, B. Mennucci, Carotenoids and light-harvesting: from DFT/MRCI to the Tamm-Dancoff approximation, J. Chem. Theory Comput. 11 (2) (2015) 655–666, https://doi.org/10.1021/ct5011246.
[24] M. Kleinschmidt, C.M. Marian, M. Waletzke, S. Grimme, Parallel multireference configuration interaction calculations on mini-β-carotenes and β-carotene, J. Chem. Phys. 130 (4) (2009) 044708, https://doi.org/10.1063/1.3062842.
[25] C.M. Marian, M. Kleinschmidt, A.R. Holzwarth, E. Ostroumov, M.G. Mu, Electronic Coherence Provides a Direct Proof for Energy-Level Crossing in Photoexcited Lutein and β-Carotene, vol. 108, (2009), pp. 1–4, https://doi.org/10.1103/PhysRevLett.103.108302 302 (September).
[26] D. Ghosh, J. Hachmann, T. Yanai, G.K.-L. Chan, Orbital optimization in the density matrix renormalization group, with applications to polyenes and β-carotene, J. Chem. Phys. 128 (14) (2008) 144117, https://doi.org/10.1063/1.2883976.
[27] A. Linden, B. Bruno, C.H. Eugster, Confirmation of the Structures of Lutein and Zeaxanthin, vol. 87, (2004), pp. 1254–1269, https://doi.org/10.1002/hlca.200490115.
[28] P.-O. Widmark, B.J. Persson, B.O. Roos, Density matrix averaged atomic natural orbital (ano) basis sets for correlated molecular wave functions, Theor. Chim. Acta 79 (6) (1991) 419–432, https://doi.org/10.1007/BF01112569.
[29] P.A. Malmqvist, A. Rendell, B.O. Roos, The restricted active space self-consistent-field method, implemented with a split graph unitary group approach, J. Phys. Chem. 94 (14) (1990) 5477–5482, https://doi.org/10.1021/j100377a011.
[30] R.S. Knox, B.Q. Spring, Dipole strengths in the chlorophylls, Photochem. Photobiol. 77 (5) (2007) 497–501, https://doi.org/10.1562/0031-8655(2003)0770497DSITC2.0.CO2.
[31] J.J.P. Stewart, Mopac2016, stewart Computational Chemistry, Colorado Springs,

(2016) URL http://openmopac.net.
[32] B.H. Besler, K.M. Merz, P.A. Kollman, Atomic charges derived from semiempirical methods, J. Comput. Chem. 11 (4) (1990) 431–439, https://doi.org/10.1002/jcc.540110404.
[33] M.W. Schmidt, K.K. Baldridge, J.A. Boatz, S.T. Elbert, M.S. Gordon, J.H. Jensen, S. Koseki, N. Matsunaga, K.A. Nguyen, S. Su, T.L. Windus, M. Dupuis, J.A. Montgomery Jr., General atomic and molecular electronic structure system, J. Comput. Chem. 14 (11) (1993) 1347, https://doi.org/10.1002/jcc.540141112.
[34] F. Aquilante, J. Autschbach, R.K. Carlson, L.F. Chibotaru, M.G. Delcey, L. De Vico, I. Fdez Galvn, N. Ferr, L.M. Frutos, L. Gagliardi, M. Garavelli, A. Giussani, C.E. Hoyer, G. Li Manni, H. Lischka, D. Ma, P.K. Malmqvist, T. Mller, A. Nenov, M. Olivucci, T.B. Pedersen, D. Peng, F. Plasser, B. Pritchard, M. Reiher, I. Rivalta, I. Schapiro, J. Segarra-Mart, M. Stenrup, D.G. Truhlar, L. Ungur, A. Valentini, S. Vancoillie, V. Veryazov, V.P. Vysotskiy, O. Weingart, F. Zapata, R. Lindh, Molcas 8: new capabilities for multiconfigurational quantum chemical calculations across the periodic table, J. Comput. Chem. 37 (5) (2016) 506–541.
[35] F. Aquilante, R. Lindh, T.B. Pedersen, Unbiased auxiliary basis sets for accurate two-electron integral approximations, J. Chem. Phys. 127 (11) (2007) 114107, https://doi.org/10.1063/1.2777146.
[36] D. Case, S. Brozell, D. Cerutti, T. Cheatham III, V. Cruzeiro, T. Darden, R. Duke, D. Ghoreishi, H. Gohlke, A. Goetz, D. Greene, R. Harris, N. Homeyer, S. Izadi, A. Kovalenko, T. Lee, S. LeGrand, P. Li, C. Lin, J. Liu, T. Luchko, R. Luo, D. Mermelstein, K. Merz, Y. Miao, G. Monard, H. Nguyen, I. Omelyan, A. Onufriev, F. Pan, R. Qi, D. Roe, A. Roitberg, C. Sagui, S. Schott-Verdugo, J. Shen, C. Simmerling, J. Smith, J. Swails, R. Walker, J. Wang, H. Wei, R. Wolf, X. Wu, L. Xiao, D. York, P. Kollman, Amber 2018, university of California, San Francisco, (2018).
[37] A.M. Rosnik, C. Curutchet, Theoretical characterization of the spectral density of the water-soluble chlorophyll-binding protein from combined quantum mechanics/molecular mechanics molecular dynamics simulations, J. Chem. Theory Comput. 11 (12) (2015) 5826–5837, https://doi.org/10.1021/acs.jctc.5b00891.
[38] I.G. Prandi, L. Viani, O. Andreussi, B. Mennucci, Combining classical molecular dynamics and quantum mechanical methods for the description of electronic excitations: the case of carotenoids, J. Comput. Chem. 37 (11) (2016) 981–991, https://doi.org/10.1002/jcc.24286.
[39] J.M. Wang, R.M. Wolf, J.W. Caldwell, P. Kollman, D. Case, Development and testing of a general amber force field, J. Comput. Chem. 25 (9) (2004) 1157–1174, https://doi.org/10.1002/jcc.20035.
[40] W.L. Jorgensen, J. Chandrasekhar, J.D. Madura, R.W. Impey, M.L. Klein, Comparison of simple potential functions for simulating liquid water, J. Chem. Phys. 79 (2) (1983) 926–935, https://doi.org/10.1063/1.445869.
[41] M.E. Madjet, A. Abdurahman, T. Renger, Intermolecular coulomb couplings from *ab initio* electrostatic potentials: application to optical transitions of strongly coupled pigments in photosynthetic antennae and reaction centers, J. Phys. Chem. B 110 (34) (2006) 17268–17,281, https://doi.org/10.1021/jp0615398.
[42] B.P. Krueger, G.D. Scholes, I.R. Gould, G.R. Fleming, Carotenoid mediated B800B850 coupling in LH2, Phys. Chem. Comm. 2 (8) (1999) 34–40, https://doi.org/10.1039/A903172C.
[43] B. Błasiak, M. Maj, M. Cho, R.W. Góra, Distributed multipolar expansion approach to calculation of excitation energy transfer couplings, J. Chem. Theory Comput. 11 (7) (2015) 3259–3266, https://doi.org/10.1021/acs.jctc.5b00216.
[44] G. Kovačćevi, V. Veryazov, Luscus: molecular viewer and editor for MOLCAS, J. Chem. Inf. 7 (1) (2015) 16, https://doi.org/10.1186/s13321-015-0060-z.
[45] V. Veryazov, P.Å. Malmqvist, B.O. Roos, How to select active space for multi-configurational quantum chemistry? Int. J. Quantum Chem. 111 (13) (2011) 3329–3338, https://doi.org/10.1002/qua.23068.
[46] A.A. Pascal, Z. Liu, K. Broess, B. van Oort, H. van Amerongen, C. Wang, P. Horton, B. Robert, W. Chang, A. Ruban, Molecular basis of photoprotection and control of photosynthetic light-harvesting, Nature 436 (7047) (2005) 134–137, https://doi.org/10.1038/nature03795.
[47] S. Santabarbara, P. Horton, A.V. Ruban, Comparison of the thermodynamic landscapes of unfolding and formation of the energy dissipative state in the isolated light harvesting complex II, Biophys. J. 97 (4) (2009) 1188–1197, https://doi.org/10.1016/j.bpj.2009.06.005.